Journal of Electroceramics (2018) 41:37–42
https://doi.org/10.1007/s10832-018-0149-7

Formation of a $KNbO_3$ single crystal using solvothermally synthesized $K_{2-m}Nb_2O_{6-m/2}$ pyrochlore phase

Woong-Hee Lee[1] · Young-Jin Ko[2] · Mir Im[2] · Sang-Hyo Kweon[1] · Sung-Hoon Cho[1] · HaiBo Xu[3] · Chong-Yun Kang[2,3] · Sahn Nahm[1,2]

Received: 5 December 2017 / Accepted: 15 June 2018 / Published online: 7 July 2018

Abstract
A $K_{2-m}Nb_2O_{6-m/2}$ single crystal with a pyrochlore phase formed when the Nb_2O_5 + x mol% KOH specimens with $0.6 \leq x \leq 1.2$ were solvothermally heated at 230 °C for 24 h. They have an octahedral shape with a size of 100 μm, and the composition of this single crystal is close to $K_{1.3}Nb_2O_{5.65}$. The single-crystal $KNbO_3$ formed when the single-crystal $K_{2-m}Nb_2O_{6-m/2}$ was annealed at a temperature between 600 °C and 800 °C with K_2CO_3 powders. When annealing was conducted at 600 °C (or with a small amount of K_2CO_3), the $KNbO_3$ single crystal has a rhombohedral structure that is stable at low temperatures (< − 10 °C). The formation of the rhombohedral $KNbO_3$ structure can be explained by the presence of the K^+ vacancies in the specimen. The $KNbO_3$ single crystal with an orthorhombic structure formed when the $K_{2-m}Nb_2O_{6-m/2}$ single crystal was annealed at 800 °C with 20 wt% of K_2CO_3.

Keywords Solvothermal synthesis · $KNbO_3$ · Single crystal · Metal vacancy

1 Introduction

The $KNbO_3$ crystal has attracted a considerable amount of interest due to its excellent nonlinear optical, ferroelectric, photocatalytic, and piezoelectric properties [1–7]. $KNbO_3$ has a cubic structure at a temperature higher than 435 °C, and the tetragonal $KNbO_3$ phase is stable at a temperature between 435 °C and 225 °C. $KNbO_3$ has an orthorhombic structure at temperatures between 225 °C and -10 °C [6–8]. Finally, the $KNbO_3$ phase has a rhombohedral structure at a temperature lower than -10 °C [6–8]. Orthorhombic $KNbO_3$ has been extensively investigated, and it exhibits excellent physical properties. Various classical methods have been used to synthesize the good quality $KNbO_3$ single crystal [3–5]. However, the process temperature of such methods is generally very high, and it is difficult to grow the good quality $KNbO_3$ single crystal using such methods due to non-stoichiometric nature, inhomogeneity and cracking [3–5].

Recently, the hydrothermal method was used to synthesize a $KNbO_3$ single crystal to overcome such problems [2, 5–11]. In general, the process temperature of the hydrothermal method is low, ranging between 120 °C and 250 °C. Moreover, the final product of the hydrothermal method has a homogeneous composition [2, 5–11]. In general, the Nb_2O_5 particles and KOH solution are used as starting materials to synthesize the $KNbO_3$ using a hydrothermal method. However, the concentration of KOH is high (6 ~ 10 M), and it is thus possible to cause serious corrosion of the reaction vessel, which can be an obstacle for industrial applications [5–11]. Furthermore, only nano-sized $KNbO_3$ single crystals have been produced using a general hydrothermal method, indicating that they are difficult for practical applications [6–11]. Micro-sized rhombohedral and orthorhombic $KNbO_3$ crystals were hydrothermally synthesized in supercritical water with very low alkaline concentrations at 400 °C [2]. Moreover, several millimeter-sized $KNbO_3$ single crystals were synthesized using a hydrothermal method, but they were produced in high KOH concentrations

Electronic supplementary material The online version of this article (https://doi.org/10.1007/s10832-018-0149-7) contains supplementary material, which is available to authorized users.

✉ Sahn Nahm
snahm@korea.ac.kr

[1] Department of Materials Science and Engineering Korea University, 145 Anam-ro, Seongbuk-Gu, Seoul 02841, Republic of Korea

[2] Nano-Bio-Information-Technology, KU-KIST Graduate School of Converging Science and Technology, Korea University, 145 Anam-ro, Seongbuk-Gu, Seoul 02841, Republic of Korea

[3] Electronic Materials Research Center, Korea Institute of Science and Technology (KIST), Seoul 02792, Republic of Korea

of 14 M at 490 °C, indicating that this method needs to be improved for practical application [5].

In this work, a $K_{2-m}Nb_2O_{6-m/2}$ single crystal, which has a pyrochlore structure with a size of 100 μm, was solvothermally synthesized at a low temperature of 230 °C with a low concentration of KOH. The orthorhombic and rhombohedral $KNbO_3$ single crystals were produced when this $K_{2-m}Nb_2O_{6-m/2}$ single crystal was annealed at 500 ~ 800 °C with a varying amount of K_2CO_3 powders, indicating that relatively large $KNbO_3$ single crystals can be easily produced. Moreover, the structural variation of the $KNbO_3$ single crystal has also been investigated in this work.

2 Experimental procedures

Analytical-grade solid potassium hydroxide and niobium oxide (> 99.9%, High Purity Chemicals, Osaka, Japan) were used as starting materials to synthesize the $K_{2-m}Nb_2O_{6-m/2}$ single crystal. At first, Nb_2O_5 (0.05 mol) was added to the solution of KOH (0.5–2.0 mol), water, and ethanol (35 mL). The volume ratio of water and ethanol is 1:1, and this mixture solution was stirred for 1 h, poured into a Teflon vessel (100 mL) and placed in an autoclave. The autoclave was heated at 230 °C for 24 h and filtered, washed with distilled water and dried at 80 °C for 12 h. Finally, the $K_{2-m}Nb_2O_{6-m/2}$ single crystals were annealed at 500 - 800 °C for 6 h with a varying amount of K_2CO_3 (0–30 wt%) to synthesize the $KNbO_3$ single crystals. The structural properties of the specimens were examined via X-ray diffraction (XRD; Rigaku D/max-RC, Tokyo, Japan) using Cu-Kα radiation, and scanning electron microscopy (SEM; Hitachi S-4300, Osaka, Japan) was used to investigate the morphology of the specimens. The composition of the specimens was investigated using an energy-dispersive X-ray spectroscope (EDS: EMAX, Horiba, Kyoto, Japan) attached to a SEM. Fourier transform infrared spectrometry (FT-IR; Thermo Fisher Scientific Nicolet iS50, USA) was used to identify defects in the $KNbO_3$ single crystal. FTIR spectra were obtained at a resolution of 4 cm^{-1} and with 32 scans per specimen. The electron mapping images of the $K_{2-m}Nb_2O_{6-m/2}$ and $KNbO_3$ single crystals were obtained using electron probe X-ray microanalysis (EPMA: JXA-8500F, Miami, U.S.A) to analyze the crystallinity and compositional homogeneity of the specimens.

3 Results and discussion

Figure 1(a)-(e) show the XRD patterns of the Nb_2O_5 + x mol% KOH specimens with $0.5 \le x \le 2.0$ solvothermally heated at 230 °C for 24 h. The $K_{2-m}Nb_2O_{6-m/2}$ (JCPDS #35–1464) pyrochlore phase was formed in the specimen with x = 0.5, but the $K_4Nb_6O_{17}$ (JCPDS #76–0977) secondary phase was

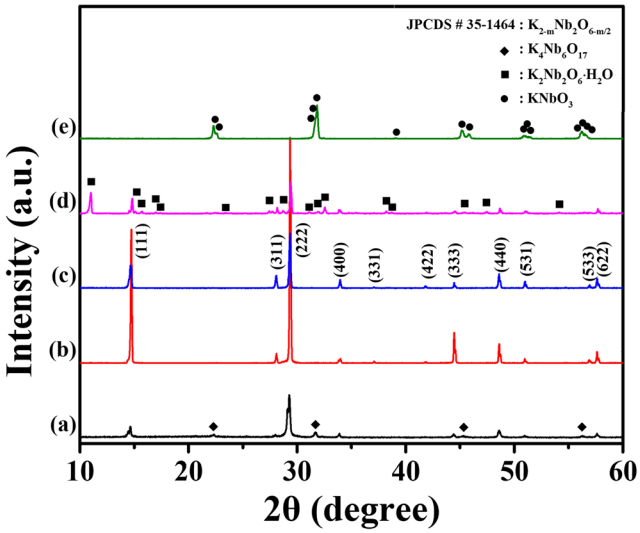

Fig. 1 XRD patterns of the Nb_2O_5 + x mol% KOH specimens heated at 230 °C for 24 h: (**a**) x = 0.5, (**b**) x = 0.6, (**c**) x = 1.2, (**d**) x = 1.5, and (**e**) x = 2.0

also developed in this specimen (see Fig. 1(a)). A pure $K_{2-m}Nb_2O_{6-m/2}$ pyrochlore phase was obtained in the specimen with x = 0.6, and this phase was maintained for a specimen with x = 1.2, as shown in Fig. 1(b) and (c). The $K_{2-m}Nb_2O_{6-m/2}$ pyrochlore phase show a high intensity (*l l l*) reflections (*l* = 1, 2, 3), indicating that it has a large (111) plane. However, the $K_2Nb_2O_6{\cdot}H_2O$ phase formed for specimens with $1.3 \le x \le 1.5$ (see Fig. 1(d)), and it changed to a $KNbO_3$ phase for the specimen with x = 2.0, as shown in Fig. 1(e) [12]. The Nb_2O_5 + x mol% KOH specimens with $0.5 \le x \le 2.0$, which were solvothermally heated at 230 °C for 24 h, were investigated using SEM, as shown in Fig. 2(a)-(d). Specimens with $x \le 1.2$, which have a $K_{2-m}Nb_2O_{6-m/2}$ pyrochlore phase, have an octahedral shape with a large (111) plane, as shown in Fig. 2(a) and (b). On the other hand, the $K_2Nb_2O_6{\cdot}H_2O$ (x = 1.5) and $KNbO_3$ (x = 2.0) specimens show nanorods and nanoparticles shapes, respectively, as shown in Fig. 2(c) and (d). The $K_{2-m}Nb_2O_{6-m/2}$ specimens are considered to be a single crystal because grain boundaries were not observed in the EPMA image of the specimen with x = 1.0 (see Fig. 2(e)). Moreover, K^+ and Nb^{5+} ions are homogeneously distributed in this specimen. The size of the $K_{2-m}Nb_2O_{6-m/2}$ single crystal with x = 0.5 is approximately 30 μm, and it increased with an increase of x to 100 μm for the specimen with x = 1.2, indicating that the size of the $K_{2-m}Nb_2O_{6-m/2}$ single crystal can be further increased by controlling the process conditions. The ratio of K^+ and Nb^{5+} ions in the $K_{2-m}Nb_2O_{6-m/2}$ single crystal is approximately 2: 3, as shown in Fig. S1 a in supplemental material 1, indicating that the $K_{1.3}Nb_2O_{5.65}$ pyrochlore phase was developed in specimens with $0.6 \le x \le 1.2$. Furthermore, the ratios of K^+ and Nb^{5+} ions in the $K_2Nb_2O_6{\cdot}H_2O$ nanorods (x = 1.5) and $KNbO_3$ nanoparticles (x = 2.0) are approximately 1: 1 and

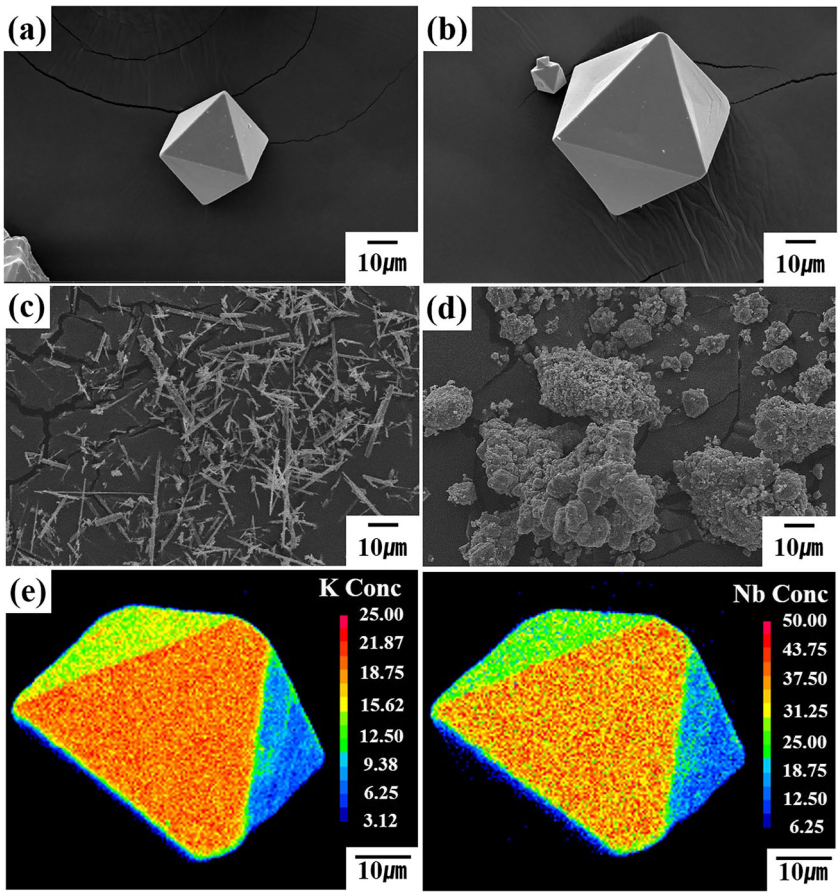

Fig. 2 SEM images of the Nb_2O_5 + x mol% KOH specimens heated at 230 °C for 24 h: (**a**) x = 0.5, (**b**) x = 1.2, (**c**) x = 1.5, and (**d**) x = 2.0. (**e**) EPMA image of the specimen with x = 1.0 showing the homogeneous distributions of K^+ and Nb^{5+} ions

1.1: 1, respectively, as shown in Figs. S1(b) and (c) in supplemental material 1. Therefore, the morphology of the specimen is considered to be influenced by the ratio of K^+ and Nb^{5+} ions.

The $K_{2-m}Nb_2O_{6-m/2}$ specimen was annealed at various temperatures with varying amounts of K_2CO_3 powders to synthesize the $KNbO_3$ single crystal by supplying K_2O to the $K_{2-m}Nb_2O_{6-m/2}$ phase. Figure 3(a)-(d) show the XRD patterns of the $K_{2-m}Nb_2O_{6-m/2}$ specimen annealed at various temperatures for 6 h with 30 wt% K_2CO_3 powders. The $K_{2-m}Nb_2O_{6-m/2}$ phase was maintained in the specimen annealed at 500 °C (see Fig. 3(a)), but a small amount of $K_4Nb_6O_{17}$ phase also formed in this specimen. Therefore, the reaction between the $K_{2-m}Nb_2O_{6-m/2}$ specimen and K_2CO_3 powders is not considered to be significant at 500 °C, but a small amount of K_2O evaporated from the $K_{2-m}Nb_2O_{6-m/2}$ specimen resulting in the formation of a $K_4Nb_6O_{17}$ secondary phase. The $KNbO_3$ phase was formed in specimens annealed at temperatures higher than 500 °C, as shown in Fig. 3(b)-(d). In general, the $KNbO_3$ ceramic has an orthorhombic structure at room temperature, but the $KNbO_3$ single crystal synthesized at 600 °C has a rhombohedral structure that can be identified by a peak at 45.5° in Fig. 3(b). The orthorhombic $KNbO_3$ phase was formed in the specimen annealed at 800 °C, as shown in Fig. 3(d) [13–16]. Moreover, both rhombohedral and orthorhombic structures are considered to coexist in the $KNbO_3$ specimen annealed at 700 °C.

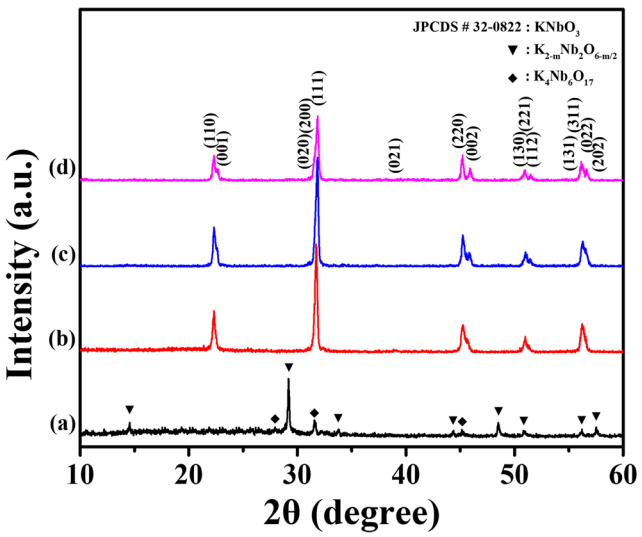

Fig. 3 XRD patterns of the $K_{2-m}Nb_2O_{6-m/2}$ specimens annealed at various temperatures for 6 h with 30 wt% K_2CO_3 powders: (**a**) 500 °C, (**b**) 600 °C, (**c**) 700 °C, and (**d**) 800 °C

For a detailed analysis of the crystal structure of the $KNbO_3$ specimens, the XRD reflections at 45.5° were measured via slow-speed scanning for specimens annealed at various temperatures, as shown in Fig. 4(a). Rhombohedral $(020)_R$ reflection was observed for specimen annealed at 600 °C, confirming that the rhombohedral $KNbO_3$ structure has developed in this specimen. The intensities of the orthorhombic $(220)_O$ and $(002)_O$ reflections increased with an increase in the annealing temperature and the orthorhombic $(220)_O$ and $(002)_O$ reflections were only observed for the specimen annealed at 800 °C, confirming that an orthorhombic $KNbO_3$ phase formed in the specimen annealed at 800 °C. Furthermore, both rhombohedral $(020)_R$ and orthorhombic $(220)_O$ and $(002)_O$ reflections were observed for the specimen annealed at 700 °C. According to a previous work, $KNbO_3$ nanorods synthesized using a hydrothermal method have a tetragonal structure that is not stable at room temperature [6, 7]. The formation of a tetragonal $KNbO_3$ phase was explained by the presence of OH^- ions in the O^{2-} sites that produced metal vacancies in the $KNbO_3$ phase [6, 7, 17]. Moreover, a rhombohedral structure was observed in the hydrothermally synthesized $KNbO_3$ particles with a small K/Nb ratio, but the presence of the unstable rhombohedral structure was not explained [2]. An FTIR analysis was conducted on the $KNbO_3$ specimens synthesized at various temperatures, as shown in Fig. 4(b). The peaks at 509 cm^{-1} and 593 cm^{-1} can be explained by the stretching vibrations of the O-Nb-O [5, 10, 18]. Multiple peaks between 1000 cm^{-1} and 1650 cm^{-1} correspond to the K-O absorption bond [19]. The intensities of multiple peaks between 1000 cm^{-1} and 1650 cm^{-1} are small for the $KNbO_3$ specimen synthesized at 600 °C, and they increased with an increase in annealing temperature. Therefore, the number of K-O bonds is considered to increase with an increase in temperature. Moreover, the EDS analysis shows that a K-deficient $KNbO_3$ phase formed in the specimen synthesized at 600 °C, and a stoichiometric $KNbO_3$ phase (or slightly K-excess $KNbO_3$ phase) formed in specimens synthesized at 700 °C (or 800 °C), as shown in Figs. S3(a)-(c) in supplemental material 2. Therefore, the presence of a rhombohedral $KNbO_3$ phase is suggested to be related to the presence of vacancies formed in the K-sites.

Figure 5(a)-(d) show the XRD patterns of a $K_{2-m}Nb_2O_{6-m/2}$ specimen annealed at 800 °C with varying amounts of K_2CO_3

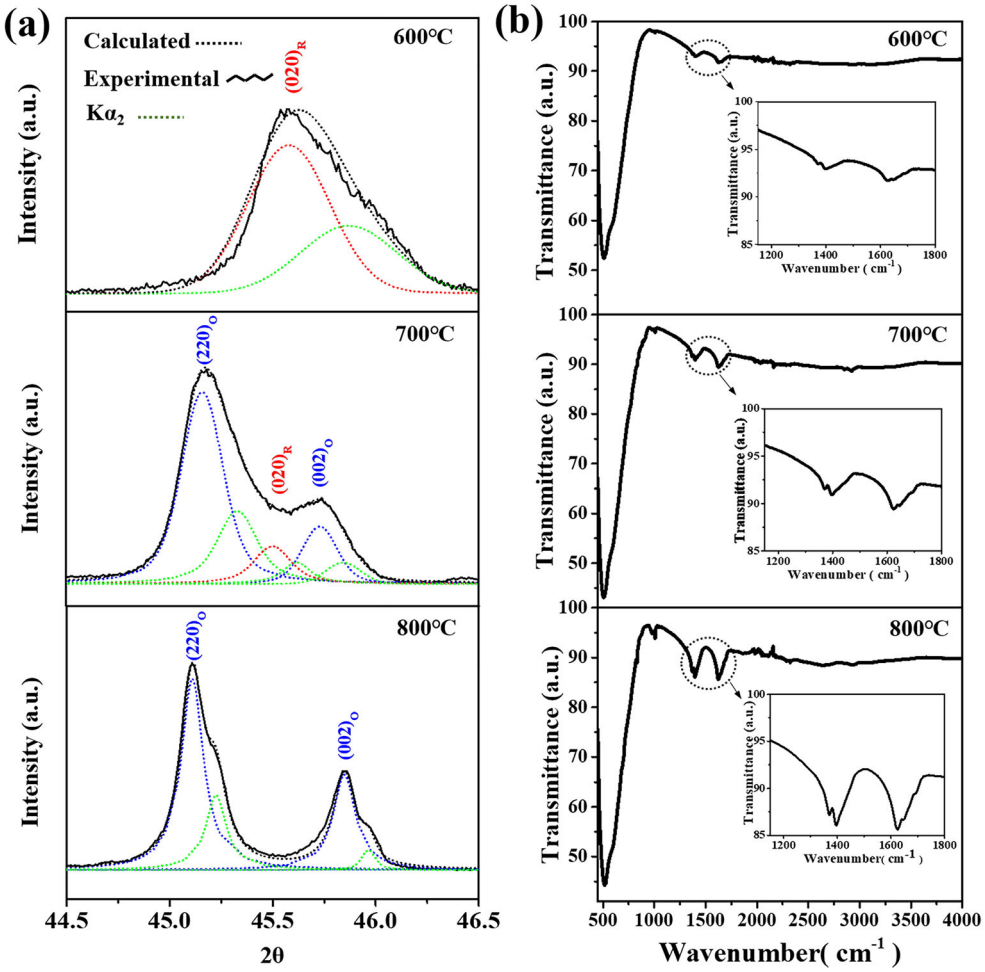

Fig. 4 (**a**) XRD reflections at 45.5° measured via slow-speed scanning and (**b**) FTIR spectra of the $KNbO_3$ specimens annealed at various temperatures for 6 h with 30 wt% K_2CO_3 powders

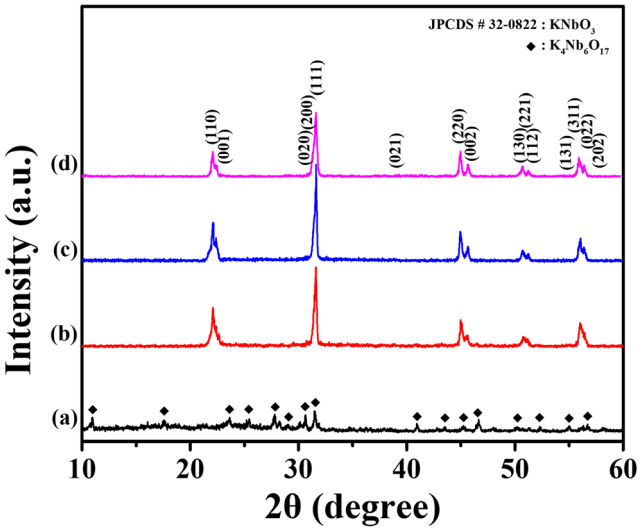

Fig. 5 XRD reflections of the $K_{2-m}Nb_2O_{6-m/2}$ specimen annealed at 800 °C with varying amounts of K_2CO_3 powders: (**a**) 0 wt%, (b) 10 wt %, (**c**) 20 wt%, and (**d**) 30 wt%

powders. The $K_4Nb_6O_{17}$ phase formed in the $K_{2-m}Nb_2O_{6-m/2}$ specimen that was annealed at 800 °C without K_2CO_3 particles, owing to the evaporation of K_2O during the annealing. The $KNbO_3$ phase formed in the specimen annealed with 10 wt% K_2CO_3 powders, but the $(220)_O$ and $(002)_O$ reflections at 45.5° were not completely separated, indicating that both rhombohedral and orthorhombic structures could form in this $KNbO_3$ phase. The $(220)_O$ and $(002)_O$ reflections were clearly separated for the specimens annealed with a large amount of K_2CO_3 powders, as shown in Fig. 5(c) and (d), indicating that they have an orthorhombic $KNbO_3$ phase [13–16]. This result also implies that the formation of rhombohedral $KNbO_3$ crystals could be related to the presence of K vacancies. Figure 6(a)-(c) show SEM images of $KNbO_3$ specimens synthesized at 800 °C with varying amounts of K_2CO_3 powders. For the specimens annealed without K_2CO_3 powders, cracks formed, probably due to the evaporation of K_2O during annealing. The $KNbO_3$ single crystal with an octahedral shape was well developed for specimens synthesized with 10 and 20 wt% K_2CO_3 powders, as shown in Fig. 6(b) and (c). However, the $KNbO_3$ single crystals were agglomerated for a specimen annealed with 30 wt% K_2CO_3 powders (see Fig. S2(d) in supplemental material 2). Figure 6(d) shows EPMA images of the $KNbO_3$ specimen synthesized with 20 wt% K_2CO_3 powders, and the homogeneous $KNbO_3$ single crystal formed without grain boundaries. Therefore, the orthorhombic $KNbO_3$ single crystal with an octahedral shape was considered to have formed when the $K_{2-m}Nb_2O_{6-m/2}$ specimen was annealed at 800 °C with 20 wt% K_2CO_3 powders, and the size of this $KNbO_3$ single crystal is approximately 100 μm.

4 Conclusions

The $Nb_2O_5 + x$ mol% KOH specimens with $0.5 \le x \le 2.0$ were solvothermally heated at 230 °C for 6 h. The single crystal with a $K_{2-m}Nb_2O_{6-m/2}$ pyrochlore structure formed for the specimens with $0.6 \le x \le 1.2$. The $K_2Nb_2O_6 \cdot H_2O$ nanorods and $KNbO_3$ nanocrystals formed for specimens with $1.3 \le x \le 1.9$ and $x = 2.0$, respectively. The $K_{2-m}Nb_2O_{6-m/2}$ single crystal has an octahedral shape with a size of 100 μm, and the composition of this single crystal is approximately $K_{1.3}Nb_2O_{5.65}$. The $K_{2-m}Nb_2O_{6-m/2}$ single crystals annealed at high temperatures (≥ 600 °C) with K_2CO_3 powders were transformed into $KNbO_3$ single crystals. The rhombohedral $KNbO_3$ single crystal was formed when the $K_{2-m}Nb_2O_{6-m/2}$ single crystal was annealed at 600 °C, probably due to the presence of K^+ vacancies in the specimen. On the other hand, the $KNbO_3$ single crystal with an orthorhombic structure was obtained when the $K_{2-m}Nb_2O_{6-m/2}$ single crystal was annealed at 800 °C.

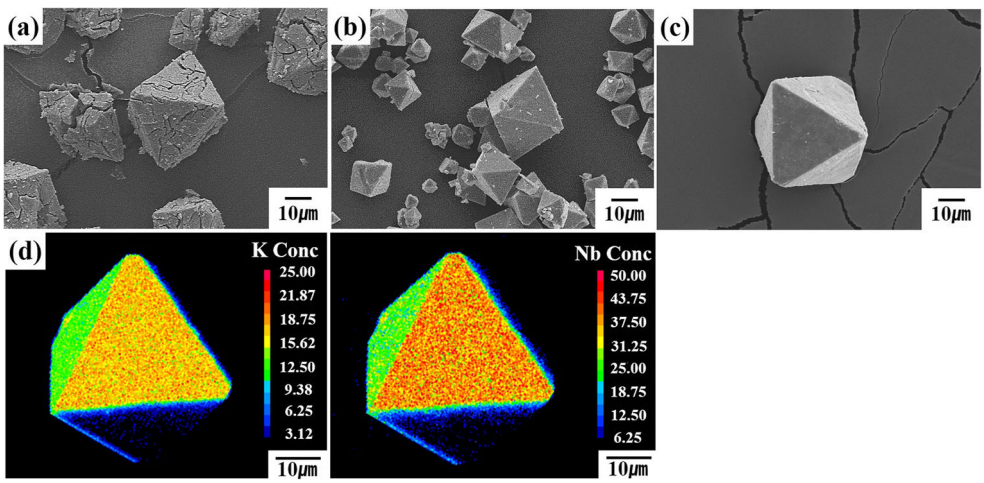

Fig. 6 SEM images of $KNbO_3$ specimens synthesized at 800 °C with varying amounts of K_2CO_3 powders: (**a**) 0.0 wt%, (**b**) 10 wt%, and (**c**) 20 wt%. (**d**) EPMA image of the $KNbO_3$ single crystal showing homogeneous distributions of K^+ and Nb^{5+} ions synthesized at 800 °C with 20 wt% K_2CO_3 powders

However, the agglomeration of $KNbO_3$ single crystals occurred when they were annealed with a large amount of K_2CO_3 ($\geq$ 30 wt%).

Acknowledgements This work was supported by the Korea Institute of Energy Technology Evaluation and Planning (KETEP) and the Ministry of Trade, Industry & Energy(MOTIE) of the Republic of Korea(No. 20152020104960). The authors also thank the Ku-Kist graduate school program of Korea University.

References

1. Y. Nakayama, P.J. Pauzauskie, A. Radenovic, R.M. Onorato, R. J. Saykally, J. Liphardt, P. Yang, Nature **447**(7148), 1098–1101 (2007)
2. B. Li, Y. Hakuta, H. Hayashi, J. Supercrit. Fluids **35**(3), 254–259 (2005)
3. V.I. Chani, K. Shimamura, T. Fukuda, Cryst. Res. Technol. **34**(4), 519–525 (1999)
4. H. Kimura, A. Miyazaki, K. Maiwa, Z.X. Cheng, C.V. Kannan, Opt. Mater. **30**(1), 198–200 (2007)
5. M. Mann, S. Jackson, J. Kolis, J. Solid State Chem. **183**(11), 2675–2680 (2010)
6. M.R. Joung, H. Xu, J.S. Kim, I.T. Seo, S. Nahm, J.Y. Kang, S.J. Yoon, J. Appl. Phys. **111**(11), 114314 (2012)
7. M.R. Joung, H. Xu, I.T. Seo, D.H. Kim, J. Hur, S. Nahm, H.M. Park, J. Mater. Chem. A **2**(43), 18547–18553 (2014)
8. S. Chakraborty, S.K. Ghosh, G.C. Das, S. Mukherjee, Int. J. Appl. Ceram. Technol. **13**(4), 743–752 (2016)
9. C. Huiqun, Y. Cheng, Y. Jie, C. Bo, X. Hong, Y. Bin, Rare Metal Mat. Eng. **45**(6), 1391–1395 (2016)
10. Y. Wang, X. Kong, W. Tian, D. Lei, X. Lei, RSC Adv. **6**(63), 58401–58408 (2016)
11. G. Shi, J. Wang, H. Wang, Z. Wu, H. Wu, Ceram. Int. **43**(9), 7222–7230 (2017)
12. X. Kong, D. Hu, P. Wen, T. Ishii, Y. Tanaka, Q. Feng, Dalton Trans. **42**(21), 7699–7709 (2013)
13. H. Tian, X. Meng, C. Hu, P. Tan, X. Cao, G. Shi, Z. Zhou, R. Zhang, Sci. Rep. **6**(1), 25637 (2016)
14. Y. Purusothaman, N.R. Alluri, A. Chandrasekhar, S.J. Kim, J. Mater. Chem. C **5**(22), 5501–5508 (2017)
15. F. Madaro, J.R. Tolchard, Y. Yu, M.A. Einarsrud, T. Grande, CrystEngComm. **13**(5), 1350–1359 (2011)
16. D.H. Kim, M.R. Joung, I.T. Seo, J. Hur, J.H. Kim, B.Y. Kim, H.J. Lee, S. Nahm, J. Eur. Ceram. Soc. **34**(16), 4193–4200 (2014)
17. N. Kumada, T. Kyoda, Y. Yonesaki, T. Takei, N. Kinomura, Mater. Res. Bull. **42**(10), 1856–1862 (2007)
18. G. Pecchi, B. Cabrera, A. Buljan, E.J. Delgado, A.L. Gordon, R. Jimenez, J. Alloys Compd. **551**, 255–261 (2013)
19. S. Kumar, L.K. Sahay, A.K. Jha, K. Prasad, Adv. Mater. Lett. **5**, 67 (2013)